On the Heterogeneity of the M Population in the Photocycle of Bacteriorhodopsin†

N. Friedman,‡ Y. Gat,‡ M. Sheves,*,‡ and M. Ottolenghi*,§

Department of Organic Chemistry, The Weizmann Institute of Science, Rehovot 76100, Israel, and Department of Physical Chemistry, The Hebrew University of Jerusalem, Jerusalem 91904, Israel

Received July 18, 1994; Revised Manuscript Received September 27, 1994⊗

ABSTRACT: The M stage in the photocycle of bacteriorhodopsin (bR), a key step in its light-induced proton pump mechanism, is studied in water/glycerol suspensions over the temperature range between 20 and −60 °C. The biexponential decay of M is analyzed for wild-type (WT) bR and for its D96N, Y185F, and D115N mutants, at various pH values, according to the scheme: bR → ($h\nu$) L → M ⇌ (k_1, k_{-1}) N → (k_2) bR. The analysis leads to the conclusion that the N state is generated, with analogous rate parameters, in all cases, including the D96N mutant. Another approach involves probing the M state, generated by steady-state illumination at −60 °C, by fast cooling to −180 °C. Subsequent irradiation with blue light, followed by gradual warming up, induces the M → ($h\nu$) M′ → bR′ → bR sequence of reactions. On the basis of characteristic difference spectra and transition temperatures observed for the M′ → bR′ process, it is concluded that the initially observed M state at −60 °C, denoted as $\{M\}_a$, is composed of three (or four) equilibrated substates, M_I, M_{II}, M_{III}, and M_{IV}. During the M → N equilibration, which corresponds to the fast phase of the M decay, $\{M\}_a$ transforms into a second state, $\{M\}_b$, in which M_{III} has been replaced by a fifth M substate, denoted as M_V. M_V is identified as the protein state in which an appropriate structural change allows reprotonation of the Schiff base, generating the N state. The low-temperature heterogeneity in M is discussed in terms of the two M states (M_1 and M_2) previously postulated [Váró, G., & Lanyi, J. K. (1990) *Biochemistry 29,* 2241] for the room temperature photocycle. The following conclusions are derived for both low and room temperature photocycles: (a) The M population is highly heterogeneous and pH dependent. (b) At least three transitions are observed between the initially formed M state and the M state that is equilibrated with N. These are assigned to protein conformational changes and to water molecule rearrangements. (c) In an aqueous suspension of WT bR at room temperature, the Schiff base reprotonation is controlled by D96. However, our results show that the formation and stability of the N state do not require the D96 residue. Moreover, at low temperatures, the $\{M\}_a \rightarrow \{M\}_b$ protein structural transformation, which has not yet been resolved at room temperature, becomes the rate-determining step in the protonation of the Schiff base.

The light-induced proton pump in bacteriorhodopsin (bR)[1] is associated with a series of transformations triggered by the primary C_{13}=C_{14}, trans → cis, isomerization of its *all-trans*-retinal chromophore, which is bound to the protein via a protonated Schiff base bond with Lys-216 [see Rothschild (1992), Lanyi (1992, 1993), Oesterhelt et al. (1992), and Ebrey (1993) for recent reviews]. The transformations are reflected by the photocycle sequence: bR $\xrightarrow{h\nu}$ K ⇌ L ⇌ M ⇌ N ⇌ O ⇌ bR in which most steps are reversible. M is the only intermediate which carries a deprotonated Schiff base, and its formation and decay during the L → M and M → N transitions appear to be the key steps in the proton translocation mechanism. Thus, accumulated evidence (see above reviews) indicates that the L → M step represents proton transfer from the protonated retinal Schiff base moiety to D85. This process induces the release of a proton from a still unidentified residue (XH) to the extracellular protein surface (Kalisky et al., 1981; Braiman et al., 1988; Otto et al., 1990; Zimanyi et al., 1992). The subsequent change in the orientation of the Schiff base, to the cytoplasmic side, leads to its reprotonation from D96, generating the N state (Otto et al., 1989; Holz et al., 1989; Gerwert et al., 1989; Butt et al., 1989; Ormos, 1991, Sasaki et al., 1992). The pump mechanism is completed by reprotonation of D96 from the cytoplasmic side, reisomerization of the retinal, and reprotonation of X^-, probably by D85.

An important finding relevant to the proton pump mechanism resulted from a kinetic analysis, which resolved the M intermediate into two sequential states, M_1 and M_2 (Váró & Lanyi, 1990, 1991a,b). It was suggested that the M_1 → M_2 step is the switch which reorients the Schiff base from the extracellular to the cytoplasmic side. Recently, the existence of at least two M states and the rate of the M_1 → M_2 transition were directly probed by studying the back-photoreaction of the M intermediate using double pulse excitation at room temperature (Druckmann et al., 1992).

† This work was supported by the James Franck Program for Laser-Matter Interactions sponsored by the Minerva Foundation and the Hebrew University of Jerusalem to M.O., and by the United States Binational Science Foundation to M.S.

‡ The Weizmann Institute of Science.

§ The Hebrew University of Jerusalem.

⊗ Abstract published in *Advance ACS Abstracts,* November 15, 1994.

[1] Abbreviations: bR, bacteriorhodopsin; D96N, bacteriorhodopsin in which aspartic acid 96 is substituted with asparagine; Y185F, bacteriorhodopsin in which tyrosine 185 is replaced with phenylalanine; D115N, bacteriorhodopsin in which aspartic acid 115 is substituted with asparagine; WT, wild type.

0006-2960/94/0433-14758$04.50/0

The back-photoreaction of M is described by the sequence: $M \xrightarrow{h\nu} M' \rightarrow bR' \rightarrow bR$, in which M′ and bR′ are deprotonated and protonated Schiff base moieties, respectively (Litvin & Balashov, 1977; Hurley et al., 1978; Kalisky et al., 1978). Since different M substates lead to distinct M′ photoproducts, the heterogeneity in M may be probed by producing M′ by a consecutive blue pulse and studying the heterogeneity in the rates and difference spectra associated with the thermal M′ → bR′ reaction (Druckmann et al., 1992). The same approach was also applied using continuous illumination of M trapped at low temperatures (Balashov & Litvin, 1981a,b; Druckmann et al., 1992). The results revealed the existence of two M substates and of multiple (sequential) bR′ species. However, the relations between the room temperature M_1 and M_2 species and the low-temperature observations remained unclear.

Aiming to obtain further insight into the heterogeneity of the M population and its implications to the proton pump mechanism, we carried out a study of the back-photoreaction of M at low temperatures. M is generated by illumination at −60 °C, stabilized by cooling to −180 °C, and then exposed to blue light excitation. The back-photoreaction is used to probe the M population in wild-type (WT) bR and in its D96N and Y185F mutants, as a function of time, prior and during its decay at −60 °C. The observations are linked to the corresponding room temperature phenomena by studying the M decay kinetics in WT bR and in the two mutants as a function of temperature in the range between 20 and −60 °C. The observations lead to several major conclusions: (a) Deprotonation of D96 is not a prerequisite for forming and stabilizing the N intermediate. (b) It is suggested that when M initiates its decay into N it is composed of an equilibrium of at least four substrates, M_I, M_{II}, M_{III}, and M_{IV}. (c) Equilibration with the N state requires a change in the M population in which the M_{III} state is replaced by a new species denoted as M_V. The $\{M_I, M_{II}, M_{III}, M_{IV}\} \rightarrow \{M_I, M_{II}, M_{IV}, M_V\}$ transition represents the structural change in the protein which allows reprotonation of the Schiff base from the cytoplasmic side generating the N state.

MATERIALS AND METHODS

Purple membranes (PM) were isolated from *Halobacterium salinarium*. The D96N, Y185F, and D115N mutants were obtained as a generous gift from Profs. R. Needleman and J. Lanyi. The membranes were suspended in 1:2 water/glycerol mixtures with 0.1 M NaCl, 10 mM Pipes buffer, and HCl or NaOH for adjusting the desired pH. Samples were light-adapted before all measurements. The samples at −180 °C were devoid of cracks, and each measurement was repeated at least 5 times to ensure reproducibility.

M Decay Kinetic Experiments. (A) Pulsed Laser Photolysis. The light-adapted sample was cooled in a Du-704 Oxford Instruments crysostat, controlled by a flow of liquid nitrogen and equipped with a Eurotherm adjusted resistive heater, and was exposed to a 532 nm, 9 ns, Nd-YAG laser. Laser-induced absorbance changes were recorded using a continuous 75W-Xe lamp, a photomultiplier, and a TDS-520 Tektronix digitizer. Data were averaged and analyzed using a PC. To avoid excitation by the white monitoring light, interference and neutral density filters were placed between the Xe lamp and the sample.

(B) Continuous Excitation Experiments. The light-adapted sample was cooled in a glass cryostat with quartz windows to the desired temperature and irradiated with a 100 W bulb through a glass filter with a cutoff of 520 nm for 10 s. The absorptions, as a function of time, were recorded by a Hewlett Packard Co. (Palo Alto, CA) 8540 diode array spectrophotometer.

Back-Photoreaction of the M Intermediate at Low Temperatures. The light-adapted sample in a 1 cm cell was cooled in a glass cryostat with quartz windows to −60 °C and irridiated with a 100 W bulb through a glass filter with a cutoff at 520 nm for 10 s. The sample was then rapidly cooled (ca. 2 min) to −180 °C by passing liquid nitrogen through the cryostat and then was irradiated through a 420 nm interference filter for 3 min and subsequently through a 610 nm cutoff filter for 2 min. Absorption spectra were recorded before and after irradiation.

To obtain thermal transformation spectra, the above irradiated sample was warmed to −150 °C, and the absorption spectrum was recorded at 60 s intervals. When no further spectral changes were observed, the sample was warmed to −140 °C, and the absorption spectrum was recorded at 60 s intervals. This routine was carried out while warming to −130 and −110 °C.

RESULTS

M Decay Kinetics in the Range between 20 and −60 °C. For studying the decay kinetics of the M intermediate over a relatively wide temperature range, we used purple membranes, as well as those of the corresponding D96N and Y185F mutants, suspended in 1:2 water/glycerol mixtures. Although affecting the M decay rate, all major features of the bR photocycle are maintained in the presence of glycerol (Kalisky et al., 1981; Cao et al., 1991). Since Y185 is located in the Schiff base linkage vicinity (Henderson et al., 1990) and D96 appears to play a key role in the decay of the M state, substitution of these groups may provide valuable information relevant to the molecular mechanism of the proton pump. Pulsed laser photolysis was used for inducing the photocycle between room temperature and −20 °C. Below −20 °C, when, due to the long M lifetime, the pulsed photolysis system becomes inadequate, the laser source was replaced by continuous illumination. Pipes buffer was chosen, since its set pH is not affected significantly by temperature changes up to ∼−60 °C. This was checked by us by monitoring a *p*-nitrophenol dye absorption (Maurel et al., 1975). Special care was taken in the case of the pulsed laser experiments, to reduce the probe beam intensity, so as to avoid back-photoreactions, i.e., bleaching of M by the 420 nm monitoring light. This was achieved by placing combinations of interference and neutral-density filters between the monitoring Xe source and the sample until a further decrease in intensity did not affect the M decay. Characteristic M decay profiles are shown in Figure 1.

At essentially all temperatures, the M decay curves for WT bR and for both D96N and Y185F mutants could not be fitted to a single exponential. As in the case of room temperature suspensions, the decay shows a biexponential profile. Consequently, we analyzed our data, adopting the widely accepted scheme (Scheme 1) at room temperature (Otto et al., 1989; Cao et al., 1991) in which $k_3 \gg k_1$, k_{-1}, k_2. The scheme accounts for the biexponential decay of M

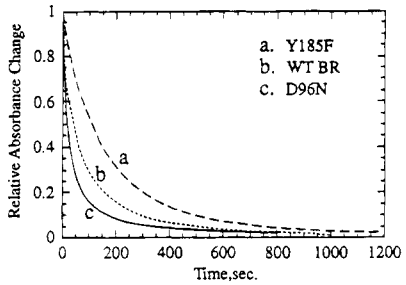

FIGURE 1: Characteristic curves showing decay of the M intermediate produced by continuous illumination at −30 °C and pH 7. For all curves, the absorbance changes are scaled to that monitored immediately after illumination, which is defined as unity. The initial changes were on the order of $\Delta OD \simeq 2 \times 10^{-1}$.

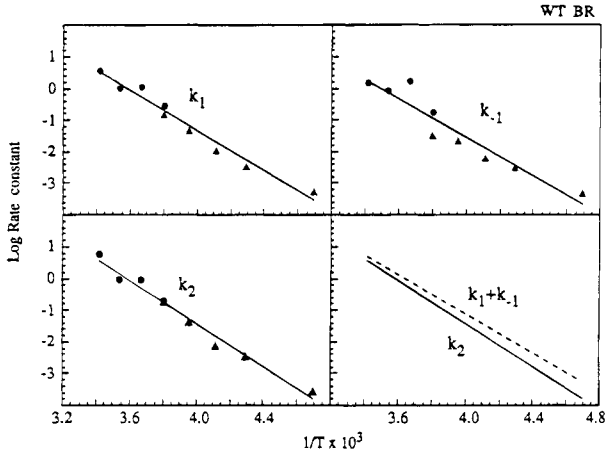

FIGURE 2: Arrhenius plots of the rate constants k_1, k_{-1}, and k_2 obtained, for WT bR, from biexponential analysis of the decay of M at pH 7. $\log(k_1 + k_{-1})$, representing the rate constant for the fast decay component, is also included. (●) Pulsed laser photolysis. (▲) Continuous illumination.

in terms of equilibration with the N intermediate (fast M decay) and subsequent relaxation to bR via the O intermediate (slow M decay). The two processes are well separated at high pH (>9) when $(k_1 + k_{-1}) \gg k_2$.

Scheme 1

$$bR \xrightarrow{h\nu} L \xrightarrow{k_3} M \underset{k_{-1}}{\overset{k_1}{\rightleftharpoons}} N \xrightarrow{k_2} bR \qquad (1)$$

The results of the kinetic analysis of the M decay profiles, according to eq 1, are shown in Figures 2−4, which present the Arrhenuis plots of the three individual rate constants, k_1, k_{-1}, and k_2, for WT bR and the two mutants at pH 7. It is evident that the biphasicity of the decay becomes clear at low temperatures when $k_2 < (k_1 + k_{-1})$. Thus, in inducing the biexponential behavior, lowering the temperature plays a role analogous to that of increasing the pH in room temperature aqueous suspensions. We note, however, that in the present water/glycerol systems a biphasic M decay is also observed (see Figure 3) in the case of the D96N mutant. This behavior will be discussed below, especially in view of previous observations (Holz et al., 1989; Miller & Oesterhelt, 1990) showing that, independently of pH, the M decay of D96 mutants in aqueous suspensions at room temperature exhibits only a single component. We also note that (at neutral pH) the room temperature M decay in D96N is slower than the wild type, while the opposite behavior is observed at −30 °C (Figure 1). The effect is due to a

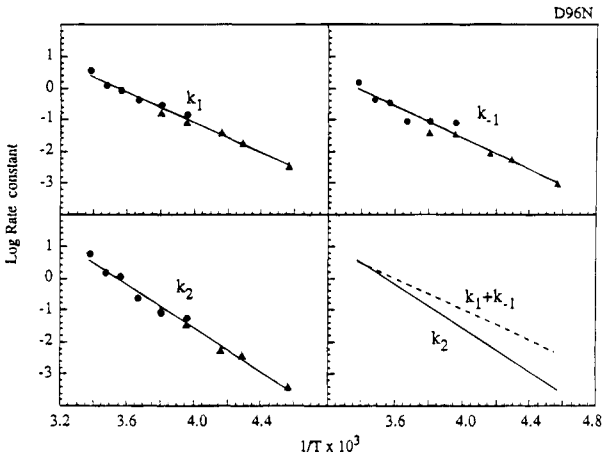

FIGURE 3: Same as for Figure 2, for the D96N mutant.

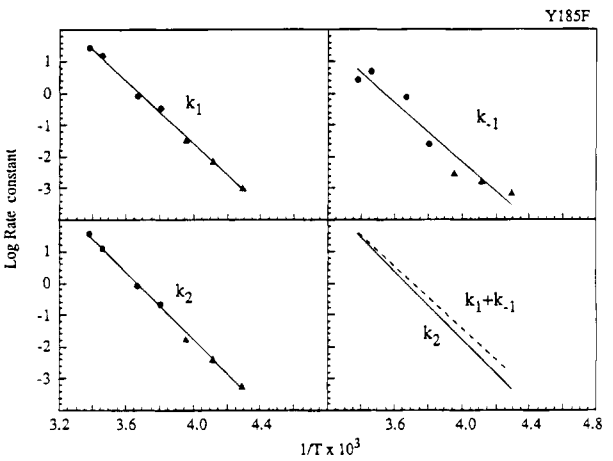

FIGURE 4: Same as for Figure 2, for the Y185F mutant.

crossing over of the respective Arrhenius plots, due to different activation energies [see Figures 2 and 3 and Tittor et al. (1989) and Cao et al. (1991)]. An analysis of the effects of pH on the rate constants k_1, k_{-1}, and k_2 was carried out at low temperatures for WT bR as well as for the D96N and Y185F mutants. As shown in Figure 5, at −30 °C, a substantial change in the values of all three rate constants is observed for WT bR and D96N between pH 6 and pH 7, with a reasonable fit to a titration-like curve characterized by an apparent pK_a of ca. 6.5. For the Y185F mutant, the effect is smaller but still detectable in the case of k_1. In this mutant, k_2 and k_{-1} show a tendency to increase at high pH.

Back-Photoreaction of the M Intermediate at Low Temperatures. (a) The Back-Photoreaction of M in WT bR at −180 °C: General Phenomena. Light-adapted purple membrane suspensions of WT bR in appropriate buffered water/glycerol solutions, cooled to −60 °C, were exposed to (λ > 520 nm) steady-state illumination, generating the M intermediate. The choice of the particular, −60 °C, temperature was an optimal compromise between higher temperatures, where the relatively fast thermal M decay interferes with the back-photoreaction studies (see below), and lower temperatures for which the L → M transition does not (or does only partially) take place. Following 10 s irradiation, the exciting light was turned off, and the samples were cooled to −180 °C. The cooling rate was faster than the M decay, allowing trapping of essentially all of the generated M intermediate. We note that although using excitation wave-

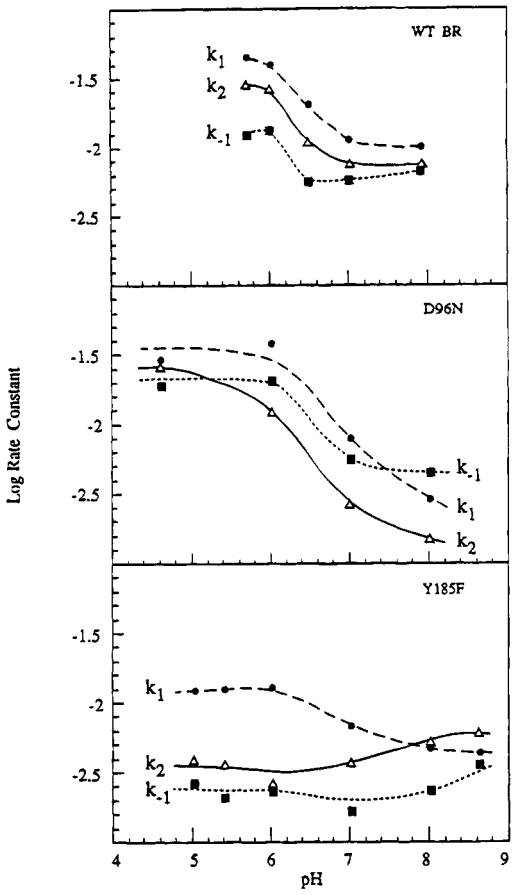

FIGURE 5: Logarithmic plots of the pH dependence of k_1, k_{-1}, and k_2 at −30 °C for WT bR, D96N, and Y185F mutants.

lengths above 520 nm, which are not absorbed by M, the bR $\xrightarrow{h\nu}$ M conversion at −60 °C could not be driven to completion. The maximal conversion fraction was ca. 35%. We attribute this observation to the back-photoreaction of a relatively long-lived intermediate absorbing above 520 nm, which generates bR. Any N or N-like species which follows M is not substantially accumulated during our exposure times, which are much shorter than the M decay, thus excluding N as the back-photoreacting species. It appears that the incomplete bR → M conversion is due to the back-photoreaction of L, which transiently accumulates during illumination. We note that irradiation at a lower pH (pH 6) further decreased the amount of M, to a conversion fraction of ca. 20%.

The back-photoreaction of M was initiated at −180 °C by exposing the above irradiated solutions to λ = 420 nm illumination using an interference filter. Since the 420 nm line is absorbed by both M and unconverted bR, the bR → K process, which leads to the characteristic red shift in absorption, was always superimposed on the spectral changes induced by excitation of M (see below). To avoid interference by the K photoproduct, we exposed the 420 nm illuminated samples to subsequent red light (λ >610 nm) irradiation, which quantitatively reconverts K to bR, eliminating the corresponding red shift. The effect of consecutive 420 nm and λ >610 nm exposures is, therefore, attributed to the net photoreaction of M.

The back-photoreaction of M is known to lead to a primary photoproduct, M′, characterized by a blue absorption similar to that of M (Litvin & Balashov, 1977; Kalisky et al., 1978, 1981; Balashov & Litvin, 1981a,b). M′ subsequently decays to bR, probably via one (or more) intermediates, denoted as bR′, absorbing similarly to bR. We followed the M′ → bR′ transitions immediately following consecutive 420 nm and >610 nm illumination at −180 °C, as well as after gradually warming the illuminated samples. The following observations were made (see Figure 6):

(I) The spectrum immediately following illumination at −180 °C was recorded and compared to that measured before illumination. As shown in Figure 6A, illumination caused an absorbance decrease around 414 nm and a corresponding increase around 560 nm. The effect is interpreted in terms of the M → M′ transition, which is accompanied by a partial decay of the M′ population (see also below). A positive sharp band around 460 nm probably originates from the difference spectrum of the M → M′ photochemical transition. The decaying M′ fraction is denoted as M'_I, and the decay process is attributed to the thermal M'_I → bR′ transition. Under the low time resolution of the continuous illumination experiments, we were unable to kinetically resolve the decay of M'_I.

(II) After completion of the M'_I → bR′ process, the sample was allowed to warm until reaching a temperature (−150 °C) where an additional absorbance change was observed (Balashov & Litvin, 1981a,b). The process is associated with a difference spectrum characterized by a 426 → 560 nm transition (Figure 6B), due to a second M′ species (M'_{II}), which is thermally more stable than M'_I. This transition, attributed to the process M'_{II} → bR′, takes place over a time scale of ca. 20 min. No further changes occur at this temperature, even after waiting for several hours. We wish to point out that the notation bR′ used for both M'_I → bR′ and M'_{II} → bR′ transitions, as well as for the decay of other M′ species (see below), does not imply that the corresponding bR′ species are exactly identical. In addition, the broad band at 560 nm, which probably includes a few bands, might indicate that the process M'_{II} → bR′ is characterized by a few transitions. It is also worthwhile noting that the quoted temperatures correspond to those of the cell holder in our cryostat and not to the actual sample temperature. It takes about 5 min for the temperature in the holder to rise, e.g., from −180 to −150 °C, and to stabilize the temperature at −150 °C (no changes in absorbances are observed during this time). Thus, the absorbance change observed after the cell holder has reached −150 °C corresponds to a sample temperature which is close to but possibly slightly lower than that of the actual reading.

(III) A third M′ species, denoted as M'_{III}, is detected upon further warming the solution to −130 °C. As shown in Figure 6C, the corresponding decay process (M'_{III} → bR′) is associated with bleaching at 420 nm and growing-in at 570 nm.

(b) pH Effects on the Relative Yields of M'_I, M'_{II}, and M'_{III}. The relative amounts of the three M′ fractions, M'_I, M'_{II}, and M'_{III}, were recorded over the 4.5−10 pH range. The pH values reported are those measured in the aqueous phase before mixing with glycerol. As shown in Figure 7, M'_I and M'_{II} show a substantial increase with decreasing pH values between pH 5 and 7, while M'_{III} shows a matching opposite pH dependency. All traces are fairly consistent with a titration-like curve characterized by an apparent pK_a of ~6.

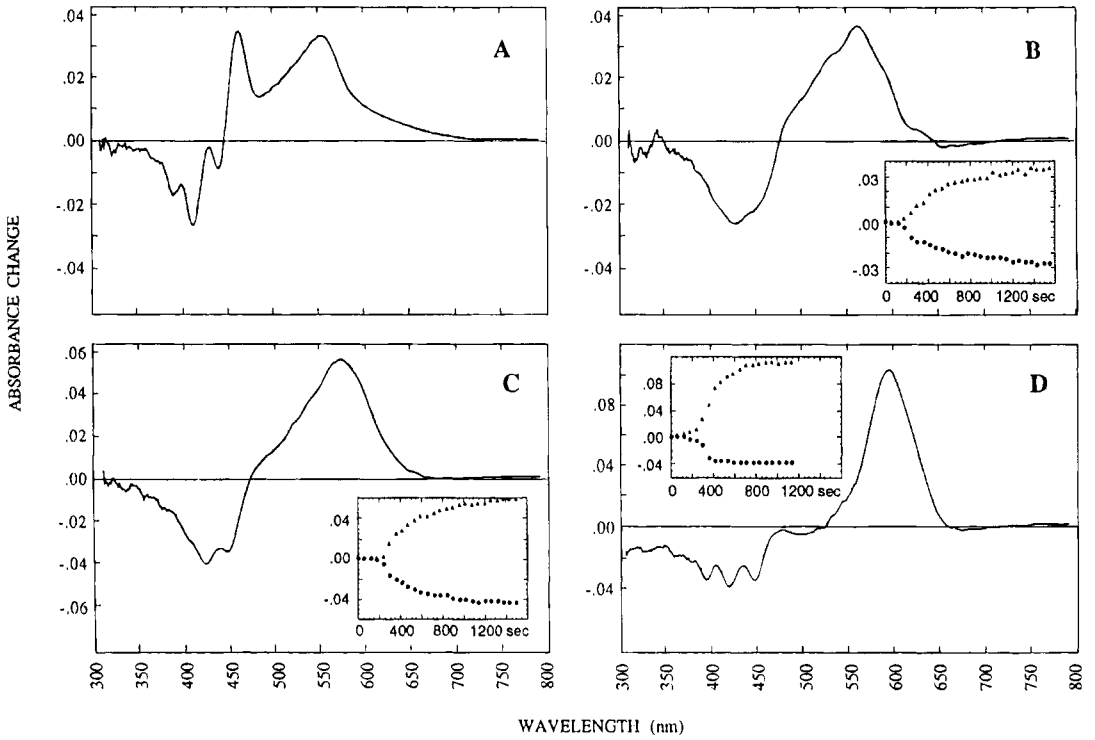

FIGURE 6: Difference spectra and corresponding kinetic traces (inserts) representing the M′ → bR′ transitions of the various M′ forms as described in the text. (A) The M'_I → bR′ transition for WT bR at −180 °C. (B) The M'_{II} → bR′ transition for WT bR at −150 °C. (C) The M'_{III} → bR′ transition for WT bR at −130 °C. (D) The M'_{IV} → bR′ transition for D96N at −110 °C. Inserts: Time evolution of the bR′ absorbance at 550−580 nm (upper trace) and decay of the M′ absorbance at 400−450 nm (lower trace). Kinetics are unresolved in the case of the M'_I → bR′ transition (A).

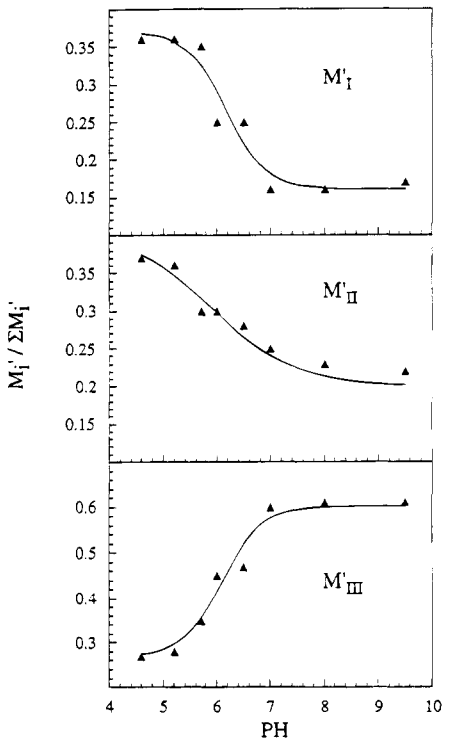

FIGURE 7: Effects of pH on the relative amounts of M'_I, M'_{II}, and M'_{III} (denoted as $M'_i/\Sigma M'_i$) for WT bR.

(c) The Back-Photoreaction of M for bR Mutants Y185F, D96N, and D115N. Back-photoreaction phenomena at −180 °C, analogous to those of bR, were also observed with both Y185F and D96N mutants. Although slightly varying in the maxima of the corresponding M′ → bR′ difference spectra (see Table 1), all three processes, M'_I → bR′, M'_{II} → bR′, and M'_{III} → bR′, occuring at temperatures essentially identical to the corresponding ones in the case of WT bR, were observed for both mutants. However, an additional feature, which is not detected in the case of the WT pigment, is the appearance of a fourth M′ species (M'_{IV}), which converts to bR′ at −110 °C (see Figure 6D and Table 1). It is possible that M'_{IV} is also present in WT bR; however, its decay is not separated from the decay of M'_{III}. The M_{IV} → bR′ transition is characterized by an increase of a sharp band at ca. 595 nm in contrast to M_{II} → bR′ and M_{III} → bR′, which were characterized by a broad band. This difference probably reflects a different decay mechanism.

As in the case of WT bR, relatively high conversion yields for the reactions were observed. In the case of Y185F, approximately 25% of the original pigment was converted to M by (λ >520 nm) steady-state illumination at −60 °C, while ~70% of M was converted to all M′ species by 420 nm illumination at −180 °C. No pH dependency studies, as detailed for WT bR, were carried out for the two mutants.

Table 1: Transition Temperatures and Corresponding Transition Wavelengths (As Detected in the Difference Spectra) Characterizing the Four M′ Substates Generated by Illumination of WT bR, Y185F, and D96N at −60 °C

M substate	transition temp (°C)	transition wavelengths (nm)		
		WT bR	Y185F	D96N
M'_I	−180	414 → 560	410 → 550	414 → 560
M'_{II}	−150	426 → 560	410 → 550	430 → 556
M'_{III}	−130	420 → 570	416 → 570	420 → 580
M'_{IV}	−110		420 → 580	422 → 600
M'_V	−140	424 → 558	414 → 550	420 → 556

Table 2: Summary of Changes Observed in the Population Ratio of M′ Substates as a Function of pH and of the M Trapping Time during Its Decay at −60 °C[a]

	WT bR				D96N				Y185F				D115N
	pH 7		pH 4.5		pH 7		pH 4.5		pH 7		pH 4.5		pH 7
substrate	100% M	30% M	100% M	30% M	100% M	30% M	100% M	30% M	100% M	70% M	100% M	70% M	100% M
M_I'	0.12	0.1	0.35	0.37	0.15	0.1	0.5	0.35	0.4	0.4	0.5	0.45	0.25
M_{II}'	0.23	0.2	0.37	0.35	0.2	0.1	0.5	0.65	0.2	0.2	0.2	0.3	0.25
M_{III}'	0.65	0.25	0.28		0.45	0.15			0.2	0.1	0.1	0.05	0.5
M_{IV}'					0.2	0.1			0.2	0.2	0.2	0.15	
M_V'		0.45		0.28		0.55				0.1		0.05	

[a] Data immediately after illumination (100% M) are compared with those in which M was trapped after ~70% decay (30% M) for WT bR and D96N, and ~30% decay for Y185F at −60 °C.

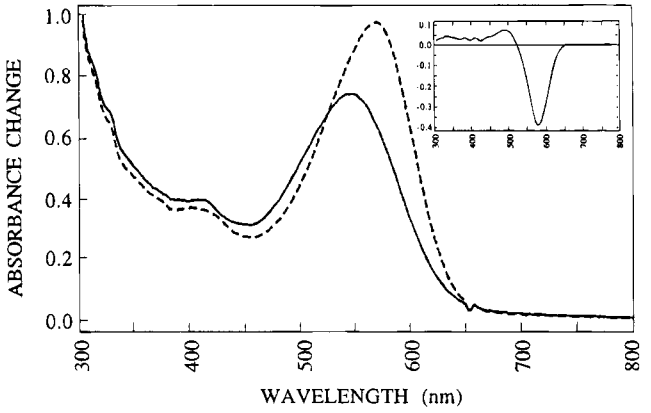

FIGURE 8: Spectral changes associated with the illumination of D115N at −60 °C (pH 7). Dashed line, before irradiation; solid line, after 10 s (λ >560 nm) illumination. Insert: the corresponding difference spectrum.

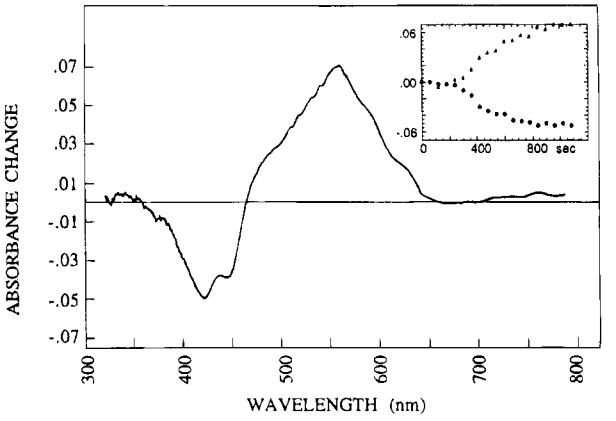

FIGURE 9: Difference spectrum and kinetic trace (insert) representing the $M_V' \rightarrow bR'$ transition at −140 °C. Data are for WT bR at pH 4.5. The back-photoreaction of M was studied in an M population trapped 500 s after termination of illumination at −60 °C.

It appears, however, that the same general trends are maintained for D96N for M_I' and M_{II}'. The data are summarized in Table 2. In the case of Y185F, decreasing the pH from 7 to 4.5 leads to an increase of ~25% in the relative amount of M_I' and a decrease of 50% in M_{III}', while the relative amounts of M_{II}' and M_{IV}' are pH independent. These changes are much smaller than those observed in the WT and D96N.

It has been suggested that in the case of the D115N mutant the rate constant of the $M_2 \rightarrow M_1$ back-reaction at room temperature is considerably faster than in the wild type, resulting in increased M_1/M_2 and L/M ratios (Zimanyi et al., 1991). With the purpose of comparing the present low-temperature data with the room temperature observations, we analyzed the M back-photoreaction of this mutant. A glycerol/water mixture of D115N at −60 °C, pH 7, irradiated for 10 s, produced a difference spectrum (Figure 8) characteristic of the bR → L transition. This L/bR mixture decayed with a half-lifetime of 35 s to a mixture of M and bR. In keeping with this observation, a 3 min irradiation produced a mixture of M and L intermediates. Illumination of this mixture with 420 nm light at −180 °C, followed by temperature elevation, revealed back-photoreaction phenomena identical to the wild type. The main data at pH 7 are summarized in Table 2.

(d) Dependence of the M′ Composition on the M Decay Time. As will be discussed below, the four M′ subspecies M_I', M_{II}', M_{III}', and M_{IV}' are interpreted in terms of a heterogeneous parent M population. In an effort to further probe the M heterogeneity during the lifetime of this intermediate, we carried out experiments in which the back-photoreaction of M at −180 °C was studied by trapping M at various times in the interval spanning its decay process at −60 °C. Thus, the time between termination of illumination at −60 °C and initiation of cooling was varied over the time scale corresponding mainly to the fast phase of the M decay. The principal observation in the case of WT bR, shown in Figure 9, is that the low-temperature trapping of *M, after initiation of its decay*, leads to a decrease in the relative amount of M_{III}' and to the formation of an additional M′ species, denoted as M_V', which was absent in the early M population trapped immediately after illumination to steady state. The $M_V' \rightarrow bR'$ process is characterized in the difference spectrum by a 424 → 558 nm spectral shift, shown in Figure 9, and by a transition temperature of −140 °C, which is intermediate between that of M_{II}' (−150 °C) and that of M_{III}' (−130 °C). The same phenomena were also observed in the cases of both Y185F and D96N mutants. As shown in Table 1, all three pigments are characterized by the same $M_V' \rightarrow bR'$ transition temperature and by similar $M_V' \rightarrow bR'$ difference spectra.

Figure 10 shows the results of the decay experiments in which the $M_V' \rightarrow bR'$ transition was monitored for WT bR, for delay times between the termination of illumination and the trapping of the M intermediate. All four photointermediates, M_I', M_{II}', M_{III}', and M_V', were probed at their corresponding decay temperature. As shown in the figure for three pH values, the decay of the relative amount of M_{III}' and the corresponding (matching) increase in the fraction of M_V' fairly match the kinetics of the fast component of the M

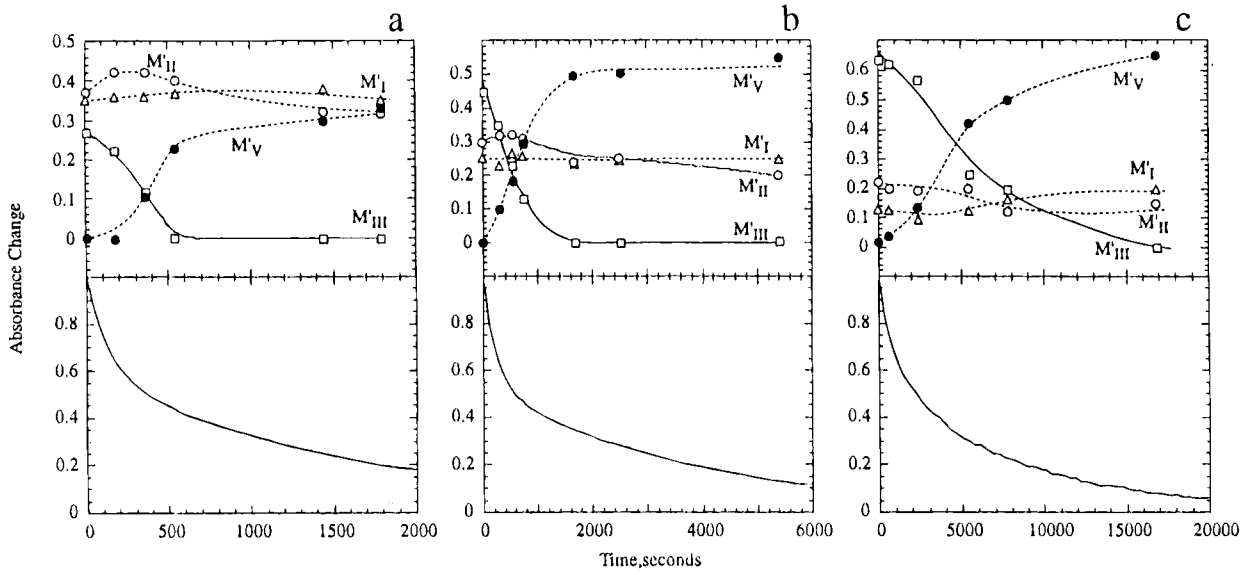

FIGURE 10: M decay traces at −60 °C, monitored at 420 nm (bottom), and time dependence of the relative amounts of the various M′ substrates (top). Time in the upper diagrams refers to the time at which the system was rapidly cooled to −180 °C after irradiation at −60 °C. (a) pH 4.5; (b) pH 6; (c) pH 7.

decay at −60 °C. This implies that cooling to a temperature in which both M decay and change in M substate composition are completely inhibited occurs substantially faster (especially at pH 7) than the decay of M at −60 °C. Analogous detailed experiments were not performed in all cases for the bR mutants. However, as shown in Table 2, for D96N (pH 7) and Y185F (pH 7 and 4.5), the principal pattern of an $M_{III} \rightarrow M_V$ transition during the initial stages of the decay of M characterizes all three pigments. We wish to point out that our claim for the identity of the rates of the fast component of the M decay and the $M_{III} \rightarrow M_{IV}$ transition is not yet backed up by a complete, quantitative, kinetic analysis. For example, at early times the M decay appears to be somewhat faster than the $M_{III} \rightarrow M_{IV}$ transition. The effect may be associated with complicating superimposed reactions such as two consecutive N forms, contribution of back M → L relaxation, etc. However, the important observation is that the qualitative match between the two processes is maintained over the whole 4.5−7.0 pH range, where both corresponding rates vary by more than an order of magnitude. This implies that the two reactions are associated with the same photocycle transformation.

DISCUSSION

M Decay Mechanism and Nature of the N State. In terms of Scheme 1, the initial component of the M decay is due to equilibration with the N intermediate. On the molecular level, the process has been attributed to protonation of the Schiff base by an intraprotein residue identified as D96 (Holz et al., 1989; Gerwert et al., 1989; Butt et al., 1989; Otto et al., 1989; Ormos, 1991; Sasaki et al., 1992). The observation that in mutants lacking the D96 residue the decay of M becomes monoexponential and also markedly pH-dependent is in keeping with this interpretation. Thus, in the absence of the internal D96 donor, reprotonation of the Schiff base occurs directly from the (cytoplasmic) bulk. Using FTIR spectroscopy, Ormos et al. (1992) provided evidence showing that in hydrated bR films the above arguments are valid only at temperatures as low as −25 °C. Below this range, the route of Schiff base reprotonation changes: Asp-85, which is on the extracellular side, replaces Asp-96 as the proton donor. It was consequently argued that proton uptake occurs from the same (extracellular) side to which it was released during M formation, resulting in no net proton pumping. This was supported by data showing that the protein conformational change manifested by a change in the intensity ratio of the two amide I bands, which is required for generating the N state, takes place only at relatively high temperatures (Ormos, 1991; Ormos et al., 1992).

An examination of the Arrhenius plots of Figure 2 does not reveal indications of a change in mechanism which may be related to the findings of Ormos et al. (1992) in the hydrated films. Thus, one would expect that a change in mechanism associated with a different reprotonation route would be reflected by changes in the Arrhenius plots of k_1, k_{-1}, and k_2. The two parameters k_1 and k_{-1} determine the equilibrium constant and the rate of equilibration between the deprotonated (M) and the subsequent reprotonated state, which should most likely be different when the reprotonating agent is Asp-96 (leading to N) or Asp-85 (leading to an L-like state). Similar arguments apply to k_2, which reflects the decay of the N state to bR, via chromophore isomerization, protein structural changes, and proton uptake from the extracellular side. We, therefore, conclude that the characteristic transition temperature postulated by Ormos and coworkers in the bR film preparations at −25 °C does not take place in our buffered glycerol/water mixtures above ∼−60 °C. This conclusion is not unreasonable in view of the differences between the film preparations and the water/glycerol mixtures, with respect to parameters that are known to affect the decay of M, primarily, the degree of hydration, pH, and salt concentration. Preliminary experiments in which irradiation at −60 °C is followed by rapid cooling, monitoring the subsequent M decay at −75 °C, show a break in the Arrhenius plots of k_1, k_{-1}, and k_2 below ∼−60 °C, which may indicate a mechanistic change. However, in the absence of corresponding FTIR data, we are presently unable to correlate these effects with the temperature-induced mechanism change suggested by Ormos (1991) and Ormos et al. (1992).

We are, therefore, led to the conclusion that the rate constants k_1, k_{-1}, and k_2 are respectively related to the generation and decay of the same N-like state over the whole −60 to 25 °C temperature range. Moreover, this applies not only to bR but also to the D96N and Y185F mutants. Of special relevance is the fact that an N-like state also occurs in the case of D96N. This implies that the thermodynamic parameters which determine the M ⇌ N equilibrium are not markedly affected by the absence of Asp-96. In WT bR, the equilibrium is associated with the structures M(SB,D96-[COOH]) and N(SBH^+,D96[COO^-]) in which SB and SBH^+ denote the unprotonated and protonated Schiff base, respectively. In D96N, the N structure lacks the negative carboxylate charge. It therefore appears that in room temperature aqueous suspensions Asp-96 affects the rate of N generation by transferring a proton to the Schiff base, but the negative charge of its carboxylate is not required for generating and stabilizing the N intermediate. In other words, the stability of the (protonated chromophore) system in N, relatively to the deprotonated M structure, appears to be determined by chromophore−protein interactions, which do not involve the deprotonated Asp-96 moiety. This picture supports the findings of Sasaki et al. (1992), which, based on FTIR studies in hydrated films of D96N bR at pH 7, led to the conclusion that a genuine N intermediate is produced by reprotonation of the Schiff base, even without the deprotonation of Asp-96. Additional independent evidence indicating that the N state is not determined by the charged state of residue 96 has been provided recently by Brown et al. (1994).

Heterogeneity of the M Population: Implications to the Photocycle Mechanism. Despite considerable controversies, accumulated evidence [see Ebrey (1993) and Lanyi (1993) for reviews] supports the extended Scheme 2 for the bR photocycle at room temperature, in which most of the transitions involve reversible steps. The original arguments for the existence of two M forms, M_1 and M_2, were based on a kinetic analysis of the photocycle (Váró & Lanyi, 1990, 1991a,b) and on the observation of a 15 nm shift in their absorption spectra in D115N bR (Váró et al., 1992). Recently (Druckmann et al., 1992), the occurrence of the two M forms in WT bR at room temperature was directly shown by applying double pulse excitation. The method allows discrimination between the two forms on the basis of different rates of the respective M′ → bR′ back-photoreactions, which occur in the 10^{-7} s time range. It was argued that the $M_1 \rightarrow M_2$ transition represents the photocycle switch, which reorients the Schiff base from the extracellular to the cytoplasmic side and raises its pK_a, allowing reprotonation (Varo & Lanyi, 1991a,b).

Scheme 2

$$bR \xrightarrow{h\nu} K \rightleftharpoons L \rightleftharpoons M_1 \xrightarrow{k_{1,2}} M_2 \underset{k_{-1}}{\overset{k_1}{\rightleftharpoons}} N \overset{k_2}{\rightleftharpoons} O \rightarrow bR \quad (2)$$

It is on this general background that the present observations associated with the heterogeneous M′ population at low temperatures should be considered. Our conclusions will be based on the basic argument that each M′ species, characterized by a distinct M′ → bR′ transition (with respect to spectral change and rate), represents a different parent M substrate. Due to the similarity of their respective spectra, these substates could not be identified, e.g., by observing changes in the spectrum of the M population itself during the M decay (i.e., during the $M_{III} \rightarrow M_V$ transition). Thus, analogously to the distinction between the two room temperature M forms, M_1 and M_2, on the basis of two different M′ species (Druckmann et al., 1992), the above five M′ species, $M'_I - M'_V$, reflect five corresponding M substates, denoted as M_I, M_{II}, M_{III}, M_{IV}, and M_V. All of these states carry a deprotonated Schiff base moiety but vary in their respective protein structure. It should be recalled that although detected by initiating the back-photoreactions at −180 °C and following them at various higher temperatures, the postulated M substates refer to the photocycle at −60 °C, i.e., at the temperature at which M was generated. The fact that moderate variations in the rate of cooling from −60 to −180 °C did not affect the observed photoreaction patterns at low temperatures is consistent with the conclusion that our relatively rapid cooling rate "froze" the M population present at the end of illumination at −60 °C. This is also in keeping with the kinetic analogy between the decay profile of M and that corresponding to the $M_{III} \rightarrow M'_V$ transition (see below). In this respect, the steady-state back-photoreaction methodology at low temperatures differs from the room temperature double pulse technique (Druckmann et al., 1992) in which the generation of M and M′ as well as the decay of M′ are all monitored at the same temperature. Scheme 3 summarizes our low-temperature observations assuming (see below) fast equilibration between the various M substates at −60 °C. It is also assumed that the equilibrium between the second set of M substates, briefly denoted as $\{M\}_b$, and N is fast relatively to the rate of the $\{M\}_a \rightarrow \{M\}_b$ transition, as well as to the decay of N to bR. These assumptions are obviously required by the simple analysis, which implies only three rate constants, k_1, k_{-1}, and k_2. Finally, it is important to point out that the five M substates detected in this work do not essentially represent all the M substates in the system. As mentioned above, due to the inherently slow warming procedure, the respective M′ → bR′ transitions could not be carried out at a strictly constant temperature. Therefore, any kinetic analysis aiming at detecting nonexponential M′ decay features, and thus additional M substates, could not be carried out.

Scheme 3

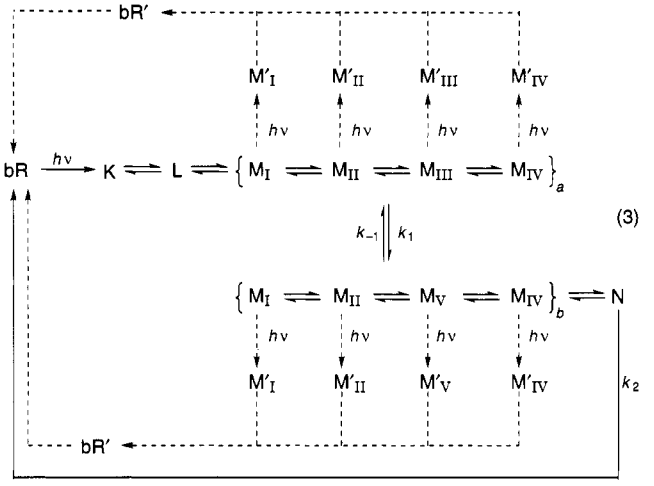

Any analysis of the mechanistic implications of the five M substates observed at low temperatures should first

consider their relationship to the two species, M_1 and M_2, postulated at room temperature. An important feature of the $M_1 \rightarrow M_2$ transition at room temperature is that it occurs during the growing-in of M, namely, on a time scale ($\sim$10 μs) which is faster, by approximately 3 orders of magnitude, with respect to the millisecond equilibration of M_2 with N. Our present studies reveal that the heterogeneous population composed of M_I, M_{II}, M_{III}, and M_{IV} (the latter being observed only in D96N and Y185F) is still present when M initiates the first stage of its decay. This would argue for the identification of the four M species as substates of M_2 (with M_1 being unresolved in our low-temperature experiments). However, the studies with D115N indicate that a mixture of M_I, M_{II}, and M_{III}, similar to that of WT bR, is present even when the L intermediate did not decay completely to M. Thus, a feasible interpretation of our data is that the low-temperature substates M_I–M_{IV}, briefly denoted as $\{M\}_a$, include both (equilibrated) M_1 and M_2 room temperature states. In other words, equilibration takes place between the four M′ states on a time scale which is faster than our time resolution. This heterogeneous low-temperature mixture includes the M_1 and M_2 states that were identified at room temperature. Support for this interpretation is associated with the effects of low pH on the relative amounts of the various M substates. It was suggested (Zimanyi et al., 1992) that at low pH (room temperature), the rate of the $M_2 \rightarrow M_1$ back-reaction increases, implying equilibration between M_1 and M_2, thereby increasing both M_1 accumulation and the L/M ratio. Our low-temperature results show an analogous behavior: At low pH, the conversion to M decreases, and, as shown in Figure 7, the amounts of M_I and M_{II} increase relatively to those M_{III}. Thus, it is suggested that M_1 consists of M_I and M_{II} while M_2 is identified with M_{III} and M_{IV}. Zimanyi et al. (1992) have also suggested that extracellular proton release takes place from a protein residue (XH), and is coupled to the reaction $M_1(XH) \rightarrow M'_1(X^-) + H^+$ (out). The pK_a of XH was determined as 5.8 and is surprisingly similar to that of the titration-like curves of Figure 7. If both processes are controlled by the same pH transition, they will identify M_I and M_{II} as preproton release states and M_{III} as the postproton release state. This point may become clear by carrying out time-resolved proton release experiments at low temperatures.

Special attention should be paid to the observation (Figure 10) that during the $M \rightarrow N$ decay the absolute amounts of the M'_I and M'_{II} substates decrease, without markedly affecting their relative amounts. This observation is in keeping with Scheme 3, which implies that the various M_i substates in $\{M\}_a$ and $\{M\}_b$ are equilibrated. In other words, while M_{III} is replaced by M_V, the relative amounts of the other substates remain practically unchanged.

Despite its high feasibility, this sequence of events (which we define as mechanism a) is not a definite interpretation of our present low-temperature and previous room temperature data. Another alternative, mechanism b, which has already been mentioned above, assumes that M_1 is not trapped in our continuous illumination experiments at low temperatures, so that the four M substates of $\{M\}_a$ are assigned to substates of M_2. Accordingly, the state $\{M\}_a$ may be denoted as $\{M\}_2$. During the $M \rightarrow N$ transition, $\{M\}_2$ transforms into the $\{M\}_b$ state, now denoted as $\{M\}_3$, which enables equilibration with N. A third alternative, mechanism c, is that the original $\{M\}_a$ population may correspond to the room temperature (RT) M_1 state, rather than to M_2. In such a case, the state defined by us as $\{M\}_b$ would correspond to M_2. This would imply that the fast phase of the M decay at -60 °C represents both $M_1 \rightarrow (k_{1,2})\ M_2$ and $M_2 \rightleftharpoons (k_1, k_{-1})$ N room temperature processes. If at -60 °C the first is the rate-determining step, namely, $k_{1,2} \ll k_1 + k_{-1}$, then the $M \rightleftharpoons N$ equilibration will be observed as a single step, in variance with the two-step ($M_1 \rightarrow M_2$ and $M_2 \rightarrow N$) process of Scheme 2 at room temperature. As stated above, this possibility is unlikely, mainly since at room temperature the $M_1 \rightarrow M_2$ transition is not correlated with the equilibration with N, namely, $k_{1,2} \gg k_1 + k_{-1}$.

Both the preferred (a) and the alternative (b) mechanisms lead to the conclusion that an additional M state ($\{M\}_b$ or $\{M\}_3$) should follows the M_2 species as observed at room temperature. Independent support to the presence of an additional M species between M_2 and N is provided by the FTIR data of Sasaki et al. (1992) carried out at room temperature with hydrated films of D96A at pH 10. With this mutant, the authors have been able to identify a new photocycle intermediate, denoted as M_N, characterized by an unprotonated Schiff base, exhibiting, however, protein structural changes similar to those of N in the photocycle of wild-type bR. We suggest that M_N is analogous to the state denoted by us as $\{M\}_b$ or $\{M\}_3$. In other words, the intermediate M_N is also present in the photocycle of WT bR. Accordingly, the $\{M\}_a \rightarrow \{M\}_b$ (or $\{M\}_2 \rightarrow \{M\}_3$) transition, which is based on the transformation of M_{III} into M_V, reflects a structural change in the protein, which allows reprotonation of the Schiff base and, thus, equilibration with the N state. It appears that this transition is slower than other transitions between the M substates and probably reflects a higher energy barrier. In view of the similarity of the M decay kinetics of WT bR and D96N (including the pH dependence), it appears that the $\{M\}_a \rightarrow \{M\}_b$ transition, rather than protonation of the Schiff base by D96, is the rate-determining step in the $M \rightarrow N$ transition at low temperatures.

As discussed above, both the decay parameters, k_1, k_{-1}, and k_2 (Figure 5), and also the ratio between the M substates in the primary set $\{M\}_a$ (Figure 7) are pH dependent. The corresponding apparent pK_a values (ca. 6.5 and ca. 6) are similar and, as mentioned above, are reminiscent of the pK_a value of the XH residue, which appears to govern the extracellular proton release process. It is tempting to suggest that all three effects are governed by the same protein residue.

The heterogeneity of the M population observed in this work is interpreted on the basis of a single bR species with branching in the photocycle at an earlier stage, leading to the various M forms. Our present data cannot confirm or disprove the role played by an initial heterogeneity in the population of bR itself, e.g., into four pH-dependent substates, as suggested by Eisfeld et al. (1993).

It is difficult at present to speculate on the specific roles of the M substates, in $\{M\}_a$ and $\{M\}_b$, in the switch mechanism which is responsible for changing the exposure and the pK_a of the protonated Schiff base. We note, however, that recent molecular dynamic simulations carried out on the M state (Dong, Schulten, and Sheves, in preparation) indicate that the M intermediate is composed of several substates. These substates are characterized by various protein conformations, especially on the cytoplasmic side of the Schiff

base vicinity, as well as by different organization of bound water molecules. Specifically, sequential changes result in the formation of a water chain connecting the Schiff base moiety to Asp96 and probably in readjusting the pK_a of these two groups. A challenge in future work will be to correlate the theortically predicted M substates with the variety of M species detected in the present study. It is evident, however, that the heterogeneity in M is higher than previously assumed and may carry important information on the switch mechanism of the proton pump in bacteriorhodopsin.

ACKNOWLEDGMENT

We thank Prof. R. Needleman and Prof. J. Lanyi for the generous gift of D96N, D115N, and Y185F mutants. We thank Prof. J. Lanyi and Prof. S. Balashov for reading the manuscript and for valuable comments.

REFERENCES

Balashov, S. P., & Litvin, F. F. (1981a) *Biophysics 26*, 566–581.

Balashov, S. P., & Litvin, F. F. (1981b) *Photobiochem. Photobiophys. 2*, 111–117.

Braiman, M. S., Mogi, T., Marti, T., Stern, L. J., Khorana, G., & Rothschild, K. J. (1988) *Biochemistry 27*, 8516–8520.

Brown, L., Yamazaki, Y., Maeda, A., Sun, L., Needleman, R., & Lanyi, J. (1994) *J. Mol. Biol. 239*, 401–414.

Butt, H. J., Fendler, K., Bamberg, E., Tittor, J., & Oesterhelt, D. (1989) *EMBO J. 8*, 1657–1663.

Cao, Y., Váró, G., Chang, M., Ni, B., Needleman, R., & Lanyi, J. K. (1991) *Biochemistry 30*, 10972–10979.

Druckmann, S., Friedman, N., Lanyi, J. K., Needleman, R., Ottolenghi, M., & Sheves, M. (1992) *Photochem. Photobiol. 56*, 1041–1047.

Ebrey, T. G. (1993) in *Thermodynamics of Membrane Acceptors and Channels* (Jackson, M., Ed.) pp 353–387, CRC Press, Boca Raton, FL.

Eisfeld, W., Pusch, C., Diller, R., Lohrmann, R., & Stockburger, M. (1993) *Biochemistry 32*, 7196–7215.

Gerwert, K., Hess, B., Soppa, J., & Oesterhelt, D. (1989) *Proc. Natl. Acad. Sci. U.S.A. 86*, 4943–4947.

Henderson, R., Baldwin, J., Ceska, T., Zemlin, F., Beckmann, E., & Downing, K. (1990) *J. Membr. Biol. 213*, 899–929.

Holz, M., Drachev, L. A., Mogi, T., Otto, H., Kaulen, A. D., Heyn, H. P., Skulachev, V. P., & Khorana, G. (1989) *Proc. Natl. Acad. Sci. U.S.A. 87*, 2167–2171.

Hurley, J., Becher, B., & Ebrey, T. G. (1978) *Nature (London) 272*, 87–88.

Kalisky, O., Lachish, U., & Ottolenghi, M. (1978) *Photochem. Photobiol. 28*, 261–268.

Kalisky, O., Ottolenghi, M., Honig, B., & Korenstein, R. (1981) *Biochemistry 20*, 649–655.

Lanyi, J. K. (1992) *J. Bioenerg. Biomembr. 24*, 169–179.

Lanyi, J. K. (1993) *Biochim. Biophys. Acta 1183*, 241–261.

Litvin, F. F., & Balashov, S. P. (1977) *Biophysics 22*, 1157–1160.

Maurel, P., Hui Bon Hoa, G., & Douzou, P. (1975) *J. Biol. Chem. 250*, 1376–1382.

Miller, A., & Oesterhelt, D. (1990) *Biochim. Biophys. Acta 1020*, 57–64.

Oesterhelt, D., Tittor, J., & Bamberg, E. (1992) *J. Bioenerg. Biomembr. 24*, 181–191.

Ormos, P. (1991) *Proc. Natl. Acad. Sci. U.S.A. 88*, 473–477.

Ormos, P., Chu, K., & Mourant, J. (1992) *Biochemistry 31*, 6933–6937.

Otto, H., Marti, T., Holz, M., Mogi, T., Lindau, M., Khorana, H. G., & Heyn, M. P. (1989) *Proc. Natl. Acad. Sci. U.S.A. 86*, 9228–9232.

Otto, H., Marti, T., Holz, M., Mogi, T., Stern, L. J., Engel, F., Khorana, H. G., & Heyn, M. P. (1990) *Proc. Natl. Acad. Sci. U.S.A. 87*, 1018–1022.

Rothschild, K. J. (1992) *J. Bioenerg. Biomembr. 24*, 147–167.

Sasaki, J., Schichida, Y., Lanyi, J. K., & Maeda, A. (1992) *J. Biol. Chem. 29*, 20782–20786.

Tittor, J., Soell, C., Oesterhelt, D., Butt, H., & Bamberg, E. (1989) EMBO *J. 8*, 3477–3482.

Váró, G., & Lanyi, J. K. (1990) *Biochemistry 19*, 2241–2250.

Váró, G., & Lanyi, J. K. (1991a) *Biochemistry 30*, 5008–5015.

Váró, G., & Lanyi, J. K. (1991b) *Biochemistry 30*, 5016–5022.

Váró, G., Zimanyi, L., Chang, M., Ni, B., Needleman, R., & Lanyi, J. K. (1992) *Biophys. J. 61*, 820–826.

Zimanyi, L., Váró, G., Chang, M., Ni, B., Needleman, R., & Lanyi, J. K. (1992) *Biochemistry 31*, 8538–8543.